Uncovering Early Galaxy Evolution in the ALMA and JWST Era
Proceedings IAU Symposium No. 352, 2019
E. da Cunha, J. Hodge, J. Afonso, L. Pentericci & D. Sobral, eds.

doi:10.1017/S1743921319008962

Properties of galaxies at $z \approx 7-9$ revealed by ALMA

Takuya Hashimoto[1,2,3]

[1]Faculty of Science and Engineering, Waseda University, 3-4-1 Okubo, Shinjuku, Tokyo 169-8555, Japan

[2]Department of Environmental Science and Technology, Faculty of Design Technology, Osaka Sangyo University, 3-1-1, Nagaito, Daito, Osaka 574-8530, Japan

[3]National Astronomical Observatory of Japan, 2-21-1 Osawa, Mitaka, Tokyo 181-8588, Japan
email: thashimoto@obsap.phys.waseda.ac.jp

Abstract. Understanding properties of galaxies in the epoch of reionization (EoR) is a frontier in the modern astronomy. With the advent of ALMA, it has become possible to detect far-infrared fine structure lines (e.g. [CII] 158 μm and [OIII] 88 μm) and dust continuum emission in star-forming galaxies in the EoR. Among these lines, our team is focusing on [OIII] 88 μm observations in high-z galaxies. After the first detection of [OIII] in the epoch of reionization (EoR) in 2016 from our team at $z = 7.21$, there are now more than ten [OIII] detections at $z > 6$ up to $z = 9.11$. Interestingly, high-z galaxies typically have very high [OIII]-to-[CII] luminosity ratio ranging from 3 to 12 or higher, demonstrating [OIII] is a powerful tracer at high-z. The high luminosity ratios may imply that high-z galaxies have low gas-phase metallicity and/or high ionization states.

Keywords. galaxies: formation — galaxies: high-redshift — galaxies: ISM

1. Introduction

1.1. *Far-infrared oxygen line as a new probe of galaxies in the reionization epoch*

Understanding properties of galaxies during reionization, at redshift $z \gtrsim 6-7$, is important. While a large number of galaxy candidates are selected with a dropout technique at $z \gtrsim 7$ owing to the Hubble Space Telescope (*HST*) and *Spitzer*/IRAC data (e.g., Ellis *et al.* 2013), the spectroscopic identifications at $z \gtrsim 7$ remain difficult (e.g., Stark *et al.* 2017 and references therein). This is mainly due to the fact that the most prominent hydrogen Lyα line is significantly attenuated by the intergalactic medium (IGM).

With the advent of the Atacama Large Millimeter/Submillimeter Array (ALMA) telescope, it has become possible to detect rest-frame far-infrared (FIR) fine structure lines in star-forming galaxies at $z > 5$ (e.g., Capak *et al.* 2015). A most commonly used line is [CII] 158 μm, which is one of the brightest lines in local galaxies (e.g., Brauher *et al.* 1998). To date, more than 21 [CII] detections are reported at $5 \lesssim z \lesssim 7$ (Carniani *et al.* 2018 and references therein).

However, based on a compiled sample with [CII] observations at $z \gtrsim 5$, Harikane *et al.* (2018) and Carniani *et al.* (2018) have revealed that [CII] may be weak for galaxies with strong Lyα emission, so-called Lyα emitters (LAEs; rest-frame Lyα equivalent widths $\mathrm{EW_0(Ly\alpha)} \gtrsim 20-30$ Å). Harikane *et al.* (2018) have interpreted the trend with photoionization models of `CLOUDY` (Ferland *et al.* 2013) implemented in spectral energy distribution (SED) models of BEAGLE (Chevallard *et al.* 2016). The authors show that low metallicity or high ionization states in LAEs lead to weak [CII]. Theoretical studies also show

that such ISM conditions lead to the decrease in the [CII] luminosity (e.g., Lagache *et al.* 2018). If we assume that $z \gtrsim 7$ galaxies in general have low metallicity or high ionization states, [CII] may not be the best line to spectroscopically confirm $z \gtrsim 7$ galaxies. Indeed, a number of null-detections of [CII] are reported at $z \gtrsim 7$ (e.g., Ota *et al.* 2014).

In fact, based on *Herschel* spectroscopy for local dwarf galaxies, Cormier *et al.* (2015) have demonstrated that [OIII] 88 μm becomes brighter than [CII] at low metallicity. Based on calculations of `CLOUDY`, Inoue *et al.* (2014) also theoretically predict that the [OIII] line at high-z should be bright enough to be detected with ALMA.

Motivated by these backgrounds, we are conducting follow-up observations of the [OIII] 88 μm line for $z > 7$ galaxies with ALMA. After the first detection of [OIII] in the reionization epoch in Inoue *et al.* (2016) at $z = 7.21$ by our team, the number of [OIII] detections is rapidly increasing. There are currently ten objects with [OIII] detections at $z \approx 6 - 9$ (Carniani *et al.* 2017; Laporte *et al.* 2017; Marrone *et al.* 2018; Hashimoto *et al.* 2018; Tamura *et al.* 2018; Hashimoto *et al.* 2019; Walter *et al.* 2018). Remarkably, Hashimoto *et al.* (2018) have detected [OIII] in a $z = 9.11$ galaxy with a high significance level of 7.4σ. These results clearly demonstrate that [OIII] is a powerful tool to confirm $z > 6 - 7$ galaxies.

1.2. *Far-infrared line luminosity ratios to diagnose properties of galaxies at $z > 7$*

Inoue *et al.* (2016) have also investigated the FIR line ratio at $z > 7$. In a combination with the null detection of [CII], the authors have shown that their $z = 7.21$ LAE has a line ratio of [OIII]/[CII] > 12 (3σ). The line ratio would give us invaluable information on properties of the interstellar medium (ISM). Given the fact that [OIII] originates only from HII regions whereas [CII] originates both from HII regions and photo-dissociated regions (PDRs), Inoue *et al.* (2016) have interpreted the high line ratio as the $z = 7.21$ LAE having highly ionized HII regions but less PDRs. Such properties would lead to a high escape fraction of ionizing photons, which is a key parameter to understand reionization. It is therefore of interest to test whether high FIR line luminosity ratios are ubiquitous for galaxies in the reionization epoch.

In this article, we will first show individual [OIII] detections. We will then discuss ubiquitously large line luminosity ratios of [OIII]/[CII] at $z = 6 - 9$ and its implications on reionization.

2. An example of our ALMA observations: MACS1149-JD1

In this section, we first show an example of our ALMA observations for MACS1149-JD1 at $z = 9.11$ (Hashimoto *et al.* 2018). For detailed observations on [OIII] and [CII], we refer the reader to Hashimoto *et al.* (2018) and Laporte *et al.* (2019), respectively.

2.1. *[OIII] 88 μm observations*

We observed MACS1149-JD1 with ALMA in Band 7 with a configuration C40-3 (ID 2015.1.00428.S, PI: A. K. Inoue). To cover the uncertainty derived from the photometric redshift analysis (e.g., Zheng *et al.* 2012), we used four setups with contiguous frequencies labeled as T3, T4, T5, and T6 encompassing the frequency range $314.4 - 340.5$ GHz and the redshift range $z = 9.0 - 9.8$. In each setup, a total bandwidth of 7.5 GHz was used, split into four spectral windows (SPWs) each with a 1.875 GHz bandwidth in the Frequency Division Mode (FDM). Each SPW has a 7.8125 MHz resolution, corresponding to a velocity resolution of ~ 7 km s^{-1}. The total on-source exposure times are 75.6, 35.3, 119.4, and 42.3 minutes, for T3, T4, T5, and T6, respectively. The T3, T4, T5, and T6 data were reduced using the CASA pipeline version 4.7.0, 4.5.2, 4.7.2, and 4.6.0,

https://doi.org/10.1017/S1743921319008962 Published online by Cambridge University Press

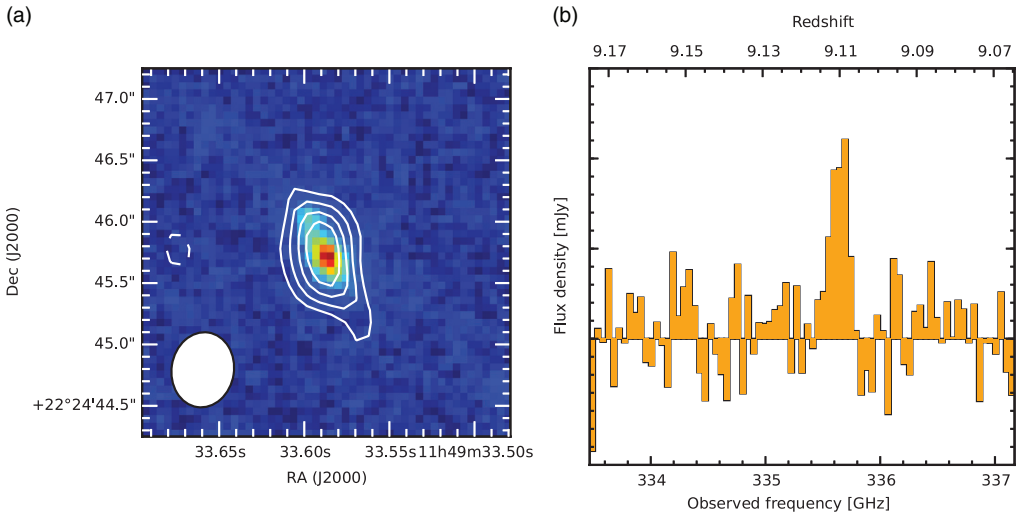

Figure 1. ALMA [OIII] contours and spectrum of MACS1149-JD1. (a) Zoom on an *HST* image (F160W) with the ALMA [OIII] contours overlaid. Contours are drawn at 1σ intervals from ± 3 to $+6\sigma$ where $\sigma = 17.5$ mJy km s^{-1} beam^{-1}. Negative contours are shown by the dashed line. Ellipse at the lower left corner indicates the synthesized beam size of ALMA. (b) ALMA [OIII] 88 μm spectrum in frequency space with a resolution of ~ 42 km s^{-1}.

respectively, with a standard calibration script provided by the ALMA observatory. We then produced final images and cubes with the `CLEAN` task using natural weighting to maximize point-source sensitivity. The spatial resolution is $0''.62 \times 0''.52$ (FWHM) and the beam position angle was PA $= -8.9°$. A quasar, J1229+0203, was used for bandpass and flux calibrations, for which a flux uncertainty is estimated to be $\lesssim 10\%$.

To search for a line, we created a data cube, six native channels of which are binned, resulting in a velocity resolution of ~ 42 km s^{-1}. In the T5 setup at ~ 335 GHz, we found a $> 3.0\sigma$ signal in five continuous binned-channels, where 1σ is the local noise estimated with the CASA task `imstat`. This frequency region is free from atmospheric absorption features. We then created a velocity-integrated intensity image between 335.5 and 335.8 GHz. The peak intensity of MACS1149-JD1 is 129.8 ± 17.5 mJy km s^{-1} beam^{-1} corresponding to a significance level of 7.4σ, where 1σ error values in this paper denote the 1σ rms or standard deviation unless otherwise specified.

The spatial centroid of the emission line is in good positional agreement with that of the UV continuum emission observed by *HST* (Figure 1, left). Both images are similarly elongated along the gravitational lensing shear. We measured the integrated line flux using the CASA task `imfit` to be 0.229 ± 0.048 Jy km s^{-1}. To obtain the redshift, we extracted the 1D-spectrum from the region with $> 3\sigma$ signals in the velocity-integrated intensity image (Figure 1, right). As can be seen, the [OIII] line is detected at around 335.6 GHz (or 893.2 μm) in the Solar system barycentric frame. Applying a Gaussian fit to the line, and with a rest-frame [OIII] frequency 3393.006244 GHz, we obtain a redshift $z = 9.1096 \pm 0.0006$ and FWHM of 154 ± 39 km s^{-1}, which is reasonable for a low mass galaxy. The integrated flux and redshift leads to an observed luminosity of $(7.4 \pm 1.6) \times (10/\mu) \times 10^7\ L_\odot$, where μ is the magnification factor. We adopt $\mu = 10$ as our fiducial lensing magnification factor.

With the CASA task `imfit`, we obtained the deconvolved size of $(0''.82 \pm 0''.25) \times (0''.30 \pm 0''.14)$. Assuming that lensing effects are equal for the major and minor axes, the intrinsic size is $(3.7 \pm 1.1)/\sqrt{\mu}$ [kpc] $\times$ $(1.4 \pm 0.9)/\sqrt{\mu}$ [kpc].

https://doi.org/10.1017/S1743921319008962 Published online by Cambridge University Press

2.2. *[CII] 158 μm observations*

After the [OIII] detection, [CII] observations were also carried out in band 5 during ALMA Cycle 6 under DDTs (2017.A.00026 and 2018.A.0004 - PI: N. Laporte). We covered a redshift range $8.96 \leqslant z \leqslant 9.16$ and a total exposure time was 6.2hrs. We used the configuration C43-4 to achieve a beam size of 0.75" × 0.63", which is similar to those used in [OIII] observations. Data were reduced using the version 5.4.0 of the CASA pipeline. We searched for line emission in a 1.5" radius circle around the UV-rest frame position (corresponding to a physical size of 13.2 kpc) and allowing a velocity offset respective to the [OIII]88μm redshift ranging from -500 km/s to 500km/s. We rebinned the data assuming a FWHM of 100km/s for [CII]158μm. No emission is detected with a 3σ upper limit on the [CII]158μm luminosity $< 3.98 \times 10^6 \times (10/\mu)\mathrm{L}_\odot$, assuming a FWHM=100km/s, with the rms measured in several beam size apertures (with $\theta_{min} = 0.63$" and $\theta_{maj} = 0.75$") distributed in a 1.5" radius circle around the UV restframe position and taking into account the best magnification($\mu = 10$).

With these observations, we obtain a luminosity ratio of $> 18.5(3\sigma)$, which is the highest among so far reported. A similar non-detection of [CII]158μm was reported by Inoue *et al.* (2016) for a Lyman-α emitter at $z = 7.2$ with [OIII]88μm emission, as well as for a $z = 8.38$ LBG with [OIII] detection.

These results clearly demonstrate that [OIII] 88 μm is a powerful tool to identify galaxies in the reionization epoch.

3. High [OIII]/[CII] luminosity ratios and implications

The line luminosity ratio, [OIII]/[CII], would give us invaluable information on chemical and ionization properties of galaxies (e.g., Inoue *et al.* 2016). For example, in local galaxies, a number of studies have examined the line ratio (e.g., Brauher *et al.* 1998). These studies have shown that dwarf metal-poor galaxies have high line ratios, [OIII]/[CII] $\approx 2 - 10$, whereas metal-rich galaxies have low line ratios, [OIII]/[CII] ≈ 0.5. Alternatively, if the ISM of galaxies is highly ionized, the [CII] luminosity would be weak because [CII] emission is predominantly emitted from the PDR (e.g., Katz *et al.* 2017).

Figure 2 summarizes the FIR line luminosity ratios of high-z galaxies (see also Laporte *et al.* 2019 for the updated data points): three $z \approx 7$ star-forming galaxies and two $z \approx 6 - 7$ sub-millimeter galaxies (SMGs). Inoue *et al.* 2016 have detected [OIII] from a $z = 7.21$ LAE with the $\mathrm{EW}_0(\mathrm{Ly}\alpha)$ value of 33 Å (SXDF-NB1006-2). With the null detection of [CII], the authors have shown that SXDF-NB1006-2 has a total line luminosity ratio of [OIII]/[CII] > 12 (3σ). Carniani *et al.* (2017) have reported detections of [OIII] and [CII] in a galaxy at $z = 7.11$ (BDF-3299). BDF-3299 has a large $\mathrm{EW}_0(\mathrm{Ly}\alpha)$ = 50 Å and thus can be categorized into LAEs. The galaxy has spatial offsets between [OIII], [CII], and UV emission. Under the assumption that both [CII] and [OIII] are associated with the UV emission, we obtain the total line ratio of 3.7 ± 0.6 using the [CII] luminosity ($4.9 \pm 0.6 \times 10^8\ L_\odot$) and the [OIII] luminosity ($18 \pm 2 \times 10^8\ L_\odot$) Hashimoto *et al.* (2018) have detected all of [OIII], [CII], and dust continuum in the two ALMA bands in a remarkably luminous LBG at $z = 7.15$. The galaxy is comprised of two UV clumps, suggesting a presence of a merger. In the whole system, the FIR luminosity ratio is 3.1 ± 0.6. Recently, Marrone *et al.* (2018) have detected both [OIII] and [CII] from a lensed SMG at $z = 6.90$ comprised of two galaxies (SPT0311-058E and SPT0311-058W). The total line luminosity ratio is 1.27 ± 0.18 and 0.56 ± 0.17 for SPT0311-058E and SPT0311-058W, respectively, where the 1σ values take the uncertainties on magnification factors into account. Finally, Walter *et al.* (2018) have detected [OIII] in an SMG at $z = 6.08$ located at the projected distance of ≈ 61 kpc from a quasar at the same redshift. In the SMG, J2100-SB, the authors have presented the line luminosity ratio of 1.58 ± 0.24 combining the previous [CII] detection.

https://doi.org/10.1017/S1743921319008962 Published online by Cambridge University Press

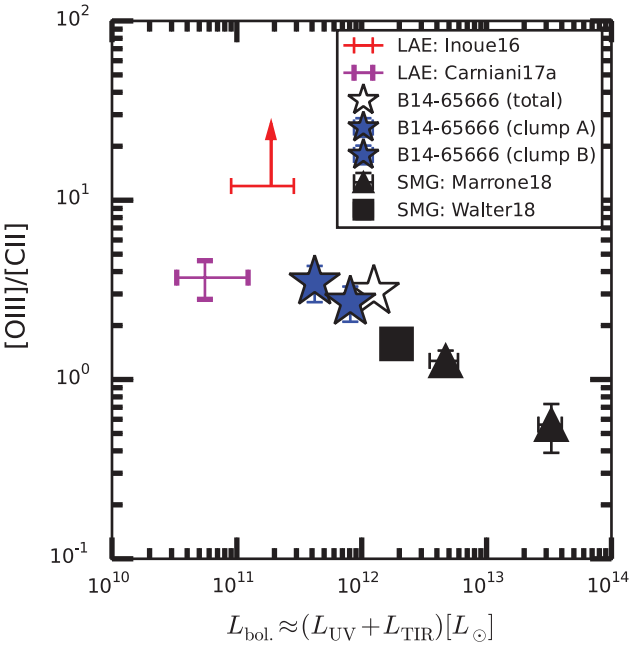

Figure 2. [OIII]-to-[CII] line luminosity ratio plotted against the bolometric luminosity estimated as the summation of the UV and IR luminosities for $z \approx 6-7$ objects. The red arrow represents the 3σ lower limit of the line luminosity ratio in the LAE of Inoue *et al.* (2016) For the two LAEs without $L_{\rm TIR}$ measurements, the upper limits of $L_{\rm bol.}$ are estimated as the summation of $L_{\rm UV}$ and the 3σ upper limits on $L_{\rm TIR}$, where we assume $T_{\rm d} = 50$ K and $\beta_{\rm d} = 1.5$. The lower limits of $L_{\rm bol.}$ for the two LAEs correspond to $L_{\rm UV}$.

Figure 2 shows a clear anti-correlation, although a larger number of galaxies are needed for a definitive conclusion. Given that the bolometric luminosity traces the mass scale of a galaxy (i.e., the stellar and dark matter halo masses and/or the SFR), the possible trend implies that lower mass galaxies having higher luminosity ratios. These would in turn indicate that lower mass galaxies have lower metallicity and/or higher ionization states (cf., Laporte *et al.* 2019).

References

Brauher, J. R., Dale, D. A., & Helou, G. 2008, *ApJS*, 178, 280
Capak, P. L., Carilli, C., Jones, G., Casey, C. M., Riechers, D., Sheth, K., Carollo, C. M., Ilbert, O., *et al.* 2015, *Nature*, 522, 455
Carniani, S., Maiolino, R., Pallottini, A., Vallini, L., Pentericci, L., Ferrara, A., Castellano, M., Vanzella, E., *et al.* 2017, *A&A*, 605, A42
Carniani, S., Maiolino, R., Amorin, R., Pentericci, L., Pallottini, A., Ferrara, A., Willott, C. J., Smit, R., *et al.* 2018, *MNRAS*, 478, 1170
Chevallard, J. & Charlot, S. 2016, *MNRAS*, 462, 1415
Cormier, D., Madden, S. C., Lebouteiller, V., Abel, N., Hony, S., Galliano, F., Rémy-Ruyer, A., Bigiel, F., *et al.* 2015, *A&A*, 578, A53
da Cunha, E., Groves, B., Walter, F., Decarli, R., Weiss, A., Bertoldi, F., Carilli, C., Daddi, E., *et al.* 2013, *ApJ*, 766, 13
Ellis, R. S., McLure, R. J., Dunlop, J. S., Robertson, B. E., Ono, Y., Schenker, M. A., Koekemoer, A., Bowler, R. A. A., *et al.* 2013, *ApJL*, 763, L7
Ferland, G. J., Porter, R. L., van Hoof, P. A. M., Williams, R. J. R., Abel, N. P., Lykins, M. L., Shaw, G., Henney, W. J., *et al.* 2013, *RMxAA*, 49, 137
Harikane, Y., Ouchi M., Shibuya, T., Kojima, T., Zhang H., Itoh, R., Ono, Y., Higuchi, R., *et al.* 2018, *ApJ*, 859, 84

https://doi.org/10.1017/S1743921319008962 Published online by Cambridge University Press

Hashimoto, T., Laporte, N., Mawatari, K., Ellis, R. S., Inoue, A. K., Zackrisson, E., Roberts-Borsani, G., Zheng, W., *et al.* 2018, *Nature*, 557, 392
Hashimoto, T., Inoue, A. K., Mawatari, K., Tamura, Y., Matsuo, H., Furusawa, H., Harikane, Y., Shibuya, T., *et al.* 2019, *PASJ* in press (arXiv:1806.00486)
Hildebrand, R. H. 1983, *QJRAS*, 24, 267
Inoue, A. K., Shimizu, I., Tamura, Y., Matsuo, H., Okamoto, T., & Yoshida, N. 2014, *ApJL*, 780, L18
Inoue, A. K., Tamura,Y., Matsuo, H., Mawatari, K., Shimizu, I., Shibuya, T., Ota, K., Yoshida, N., *et al.* 2016, *Science*, 352, 1559
Knudsen, K. K., Watson, D., Frayer, D., Christensen, L., Gallazzi, A., Michałowski, M. J., Richard, J., & Zavala, J. 2017, *MNRAS*, 466, 138
Katz, H., Kimm, T., Sijacki, D., & Haehnelt, M. G. 2017, *MNRAS*, 468, 4831
Lagache, G., Cousin, M., & Chatzikos, M. 2018, *A&A*, 609, A130
Laporte, N., Ellis, R. S., Boone, F., Bauer, F. E., Quénard, D., Roberts-Borsani, G. W., Pelló, R., Pérez-Fournon I., *et al.* 2017, *ApJL*, 837, L21
Laporte, N., Katz, H., Ellis, R. S., Lagache, G., Bauer, F. E., Boone, F., Inoue, A. K., Hashimoto, T., *et al.* 2019, *ApJL*, 487, L81
Marrone, D. P., Spilker, J. S., Hayward, C. C., Vieira, J. D., Aravena, M., Ashby, M. L. N., Bayliss, M. B., Béthermin, M., *et al.* 2018, *Nature*, 553, 51
Ota, K., Walter, F., Ohta, K., Hatsukade, B., Carilli, C. L., da Cunha, E., González-López, J., Decarli, R., *et al.* 2014, *ApJ*, 792, 34
Stark, D. P., Ellis, R. S., Charlot, S., Chevallard, J., Tang, M., Belli, S., Zitrin, A., Mainali, R., *et al.* 2017, *MNRAS*, 464, 469
Tamura, Y., Mawatari, K., Hashimoto, T., Inoue, A. K., Zackrisson, E., Christensen, L., Binggeli, C., Matsuda, Y., *et al.* 2019, *ApJ*, 874, 27
Walter, F., Riechers, D., Novak, M., Decarli, R., Ferkinhoff, C., Venemans, B., Bañados, E., Bertoldi, F., *et al.* 2018, *ApJ*, 869L, 22
Zheng, W., Postman, M., Zitrin, A., Moustakas, J., Shu, X., Jouvel, S., Host, O., Molino, A., *et al.* 2012, *Nature*, 489, 406

Discussion

A: In [CII] observations for MACS1149-JD1, did you use similar beam sizes to those used in [OIII] observations?

HASHIMOTO: Yes, we used almost the same beam sizes in the two observations. Therefore, it is unlikely that [CII] emission is partly resolved out.

SMIT: Do you see any spatial offsets between UV and dust continuum emission?

HASHIMOTO: In the case of B14-65666, an LBG at $z = 7.15$, we do not see any statistically significant spatial offset.

C: You said that some theoretical models cannot reproduce the large [OIII]-to-[CII] luminosity ratios. In those simulations, what did they assume?

HASHIMOTO: I am not sure about the details on the simulations. However, these simulated galaxies have similar SFRs and stellar masses to those of our observations. Therefore, it is likely that something is missing in these simulations.

D: Is it possible that AGN activity enhances the luminosity ratios?

HASHIMOTO: It is unlikely because, in the local Universe, the luminosity ratios are similar for AGN-dominated galaxies and normal star-forming galaxies.

https://doi.org/10.1017/S1743921319008962 Published online by Cambridge University Press